ELSEVIER

Thermochimica Acta 311 (1998) 81–86

thermochimica acta

Species-specific isoconversion effective activation energies derived by thermogravimetry–mass spectrometry

Edouard Bonnet, Robert L. White*

Department of Chemistry and Biochemistry, University of Oklahoma, Norman, OK 73019, USA

Received 8 May 1997; received in revised form 26 August 1997; accepted 15 September 1997

Abstract

The use of species-specific mass spectral ion signal temperature profiles for generating isoconversion effective activation energies by the Flynn–Wall–Ozawa method is described. Effective activation energies derived from mass-loss and mass-spectral results obtained from TG-MS analyses of calcium oxalate monohydrate and poly(vinyl butyral) thermal decompositions are compared. Although effective activation energies derived from mass-loss data may suggest changes in overall reaction processes, species-specific effective activation energy variations provide information regarding selected reaction mechanisms. © 1998 Elsevier Science B.V.

Keywords: Isoconversion activation energy; Thermogravimetry-mass spectrometry

1. Introduction

Kinetic parameters derived from thermal analysis techniques can be useful for elucidating mechanisms of thermal processes. Unfortunately, it is difficult to obtain kinetic parameters representing simultaneous processes because thermal analyses do not readily discriminate between individual mechanisms. Alternatively, simultaneous reactions can be characterized by computing effective activation energies at various conversions during a thermal event. Isoconversion activation energies reflect the relative contributions of thermal processes that occur at selected degrees of transformation [1]. Effective activation energy calculation procedures assume that a single process is responsible for thermal transformations. When a single process is indeed responsible for thermal transformation, calculated effective activation energies are constant throughout the transformation. When thermal transformation involves multiple processes, calculated effective activation energies change with degree of transformation in a manner that reflects the changing contributions of individual processes to the overall transformation.

Vyazovkin et al. [2–5] have demonstrated the use of isoconversion effective activation energy calculations for characterizing complex thermal processes and have proposed simple guidelines for interpreting the shapes of activation energy vs. conversion plots. Parallel processes with different activation energies result in an increase in the effective activation energy with increasing conversion. When a change in the rate-limiting step of a thermal process occurs during thermal transformation, effective activation energies

*Corresponding author. Tel.: 00 1 (405) 325-4806; fax: 00 1 (405) 325-6111; e-mail: rlwhite@chemdept.chem.ou.edu

PII S0040-6031(97)00411-5

decrease with increasing conversion. Isoconversion effective activation energy calculations have been used to investigate mechanisms of poly(propylene) thermal decomposition [6] and the effects of fire retardants on this decomposition [7,8], dehydration of potassium and calcium oxalate monohydrates [9], and decomposition pathways for tetrazole [10] and poly(5-vinyl tetrazole) [11].

Most previous studies involving isoconversion effective activation energy calculations have employed thermogravimetry for thermal analysis. However, as Ozawa and Kanari [12] have suggested, isoconversion calculations based on results obtained by species-specific thermal analysis should provide more information regarding complex thermal processes. Although Vyazovkin et al. [6] previously employed mass spectrometry to study poly(propylene) thermal decomposition pathways, their results merely confirmed those obtained by mass-loss measurements and did not provide additional information regarding reaction mechanisms. We describe here procedures for calculating species-specific isoconversion effective activation energies from ion-signal temperature profiles obtained by thermogravimetry–mass spectrometry (TG-MS) analyses.

2. Experimental

TG-MS measurements were made by connecting the gas outlet of a Du Pont (Wilmington, DE) Model 951 TG analyzer to a Hewlett–Packard (Palo Alto, CA) 5985 quadrupole mass spectrometer by using a Scientific Glass Engineering (Austin, TX) MCVT-1-50 variable splitting valve. The 25 cm long TG-MS fused silica transfer line and splitter valve were contained within an oven that was maintained at 473 K during analyses. Electron-bombardment ionization mass spectra (70 eV) were obtained at rates between 8 and 20 spectra/min, depending on the TG heating rate employed. During TG analysis, ≈10 mg samples were heated at nominal rates of 10, 15 and 25 K/min in platinum sample pans. TG-MS analyses were performed in duplicate, and information derived from six analyses were employed for isoconversion effective activation energy calculations. TG samples were heated in flowing helium and the variable splitter valve was adjusted to maintain mass-spectrometer ion source pressures of ca. 3×10^{-5} torr during TG-MS analyses.

Calcium oxalate monohydrate (99.9995% purity) was obtained from Johnson Matthey (Ward Hill, MA). Poly(vinyl butyral) (MW $1.5–3.0\times10^5$) was obtained from Hitachi (Hitachi City, Japan). Helium (99.9995%) was purchased from Union Carbide, Linde Division (Danbury, CT).

3. Results and discussion

To calculate species-specific isoconversion effective activation energies from TG-MS mass-spectral data, it is necessary to correlate the time dependence of ion signals with TG sample temperatures. The TG analyzer data system provided the capability of measuring elapsed time and sample temperature, in addition to sample mass. By using GC/MS software to operate the mass spectrometer, it was possible to record elapsed times with mass spectra during TG-MS analyses. By simultaneously starting the TG and MS data systems, it was possible to correlate mass spectra with TG sample mass and temperature. However, the fact that TG effluent had to pass through the TG-MS interface, before reaching the mass-spectrometer ion source, introduced a delay between sample mass-loss and mass-spectrometric detection of volatiles responsible for the mass loss. By correlating the derivative of the dehydration mass-loss curve obtained by TG analysis of calcium oxalate monohydrate with the m/z 18 (water molecular ion) mass-spectral ion signal temperature profile obtained by mass-spectrometric analysis of TG effluent, this delay time was measured. Fig. 1 shows overlaid plots of inverted TG mass-loss curve derivatives (solid lines) and m/z 18 ion signal temperature profiles (broken lines) obtained with the TG helium purge gas flow rate adjusted to 100, 150 and 200 ml/min. For each of the plots in Fig. 1, the m/z 18 ion signal time axis was shifted until it coincided with the mass-loss derivative profile. The m/z 18 ion signal profile obtained by using a 100 ml/min He purge gas flow rate was shifted by subtracting 9 s from measured elapsed times. For m/z 18 ion signal profiles measured by using 150 and 200 ml/min He purge gas flow rates, 7.2 and 6 s, respectively, were subtracted to match these profiles with TG derivatives.

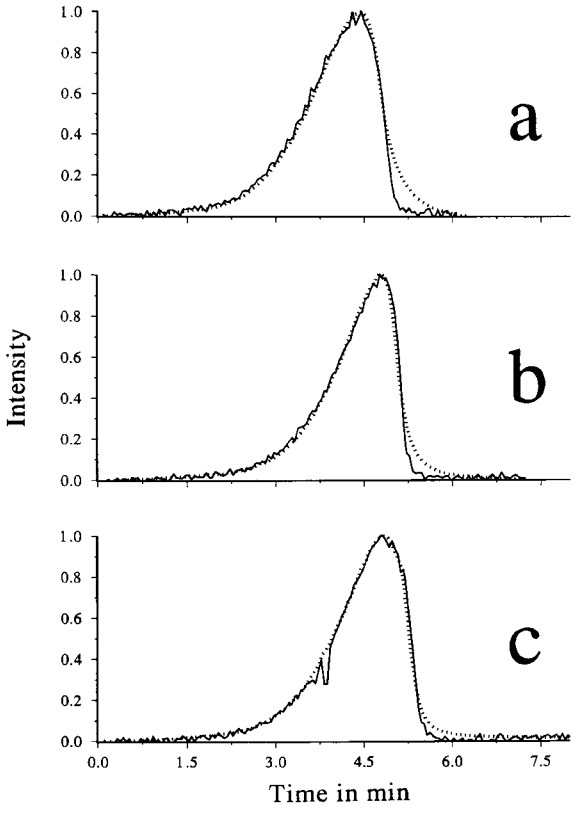

Fig. 1. TG-MS mass-loss derivatives (solid lines) and *m/z* 18 ion signal profiles (broken lines) obtained with helium purge gas flow rates of (a) 100, (b) 150 and (c) 200 ml/min for dehydration of calcium oxalate monohydrate.

The tailing portions of the TG mass-loss derivatives and *m/z* 18 ion signal profiles in Fig. 1 do not match as well as the leading portions. However, the coincidence of the tailing portions of these curves improved as the He flow rate was increased. This suggests that transport of TG effluent through the mass-spectrometer ion source was less efficient when lower He purge gas flow rates were employed. Based on these findings, a TG helium purge gas flow rate of 200 ml/min was selected for subsequent TG-MS measurements. TG-MS ion signal elapsed times were corrected before calculating sample temperatures by subtracting 6 s, which was the time required for TG effluent to reach the mass-spectrometer ion source.

Calcium oxalate monohydrate thermal decomposition consists of three well-separated mass-loss steps that involve evolution of single species during each step [5,13]. To evaluate the use of TG-MS mass-spectral results for species-specific kinetic calculations, effective activation energies derived from mass-loss and mass-spectral ion signal temperature profiles obtained from TG-MS analyses of calcium oxalate monohydrate were compared. Effective activation energies were computed from TG mass-loss information at 0.5% conversion intervals for water, carbon monoxide, and carbon dioxide evolutions by using the Flynn–Wall–Ozawa method [14].

Isoconversion effective activation energies calculated from mass-loss (solid line) and integrated *m/z* 18 ion signal (broken line) temperature profiles corresponding to evolution of water are shown in Fig. 2. These isoconversion activation energy curves exhibit similar shapes, but the curve derived from mass-spectral ion signal temperature profiles is lower by ca. 4 kJ mol^{-1}. Isoconversion effective activation energies calculated from mass-loss (solid line) and integrated *m/z* 28 ion signal (broken line) temperature profiles corresponding to CO evolution are shown in Fig. 3. Again, the curves exhibit similar shapes but are not coincident. The curve derived from mass-spectral ion signal temperature profiles is ca. 4–6 kJ mol^{-1} higher than the mass-loss derived curve. Isoconversion effective activation energies calculated from mass-loss (solid line) and integrated *m/z* 44 ion signal (broken line) temperature profiles corresponding to CO_2 evolution are shown in Fig. 4. The correlation between mass-loss and mass-spectral ion signal tem-

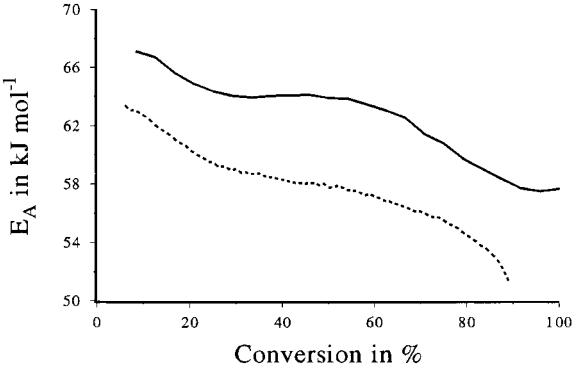

Fig. 2. Variations of effective activation energies derived from water mass-loss (solid line) and *m/z* 18 mass-spectral ion signal temperature profiles (broken line) for the thermal decomposition of calcium oxalate monohydrate.

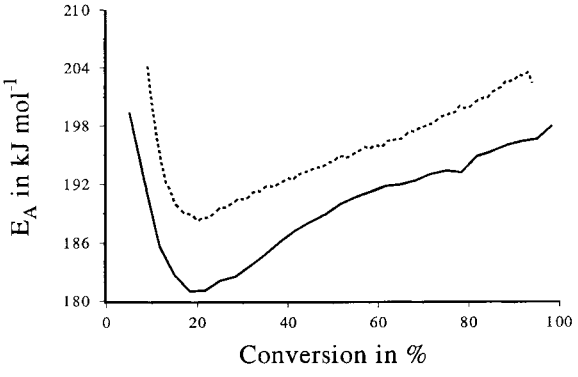

Fig. 3. Variations of effective activation energies derived from CO mass-loss (solid line) and *m/z* 28 mass-spectral ion signal temperature profiles (broken line) for the thermal decomposition of calcium oxalate monohydrate.

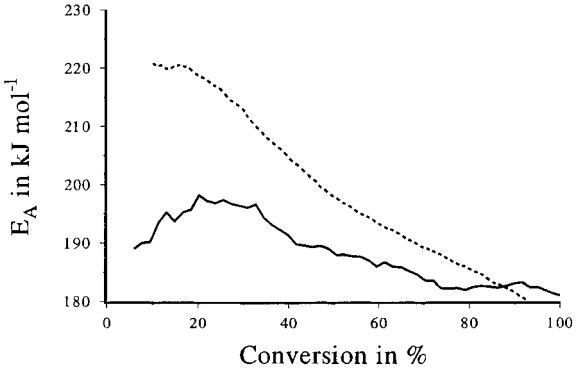

Fig. 4. Variations of effective activation energies derived from CO_2 mass-loss (solid line) and *m/z* 44 mass-spectral ion signal temperature profiles (broken line) for the thermal decomposition of calcium oxalate monohydrate.

perature profile derived activation energies is not as good as for dehydration and CO evolution. At low conversions, activation energies derived from mass-spectral ion signal temperature profiles were as much as 30 kJ mol^{-1} higher than those derived from mass-loss profiles. This was most likely caused by variations in the background *m/z* 44 ion signal during TG-MS analyses, which distorted ion signal temperature profiles. The 4–6 kJ mol^{-1} separation between isoconversion activation energies calculated from mass-loss and mass-spectral ion signal temperature profiles associated with dehydration and CO evolution is consistent with expected measurement errors. However, the fact that effective activation energy curves had similar shapes for dehydration and CO evolution suggests that errors were systematic rather than random. Differences in TG balance and MS detector response functions may have contributed to these systematic offsets.

Isoconversion effective activation energies were also calculated from results of TG-MS analyses of poly(vinyl butyral) thermal decomposition. Poly(vinyl butyral) (PVB) is used as a ceramic binder for non-oxidative ceramic sintering. Commercial grade PVB is manufactured by converting poly(vinyl acetate) to poly(vinyl alcohol) and then reacting this polymer with butanal. This process does not lead to complete conversion to poly(vinyl butyral), but, instead, results in a multifunctional polymer containing residual acetate and hydroxyl groups:

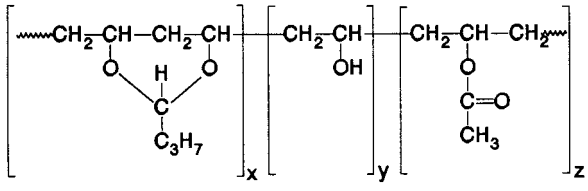

The composition of commercial grade PVB is typically: x>75%, y=18–22%, and z<3%. Thus, PVB decomposition proceeds via multiple pathways involving different polymer functionalities. TG-MS mass-selected ion signal temperature profiles and the mass-loss curve obtained by heating a PVB sample at 10 K/min are shown in Fig. 5. Ion signals corresponding to *m/z* 18, 60, 72, and 91 were found by our

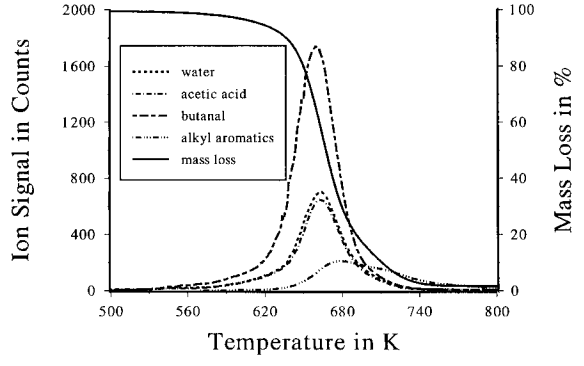

Fig. 5. Mass-loss curve and species-specific mass-spectral ion signal temperature profiles obtained by TG-MS analysis of a PVB sample heated at 10 K/min.

previous studies to be representative of water, acetic acid, butanal, and alkyl aromatics, respectively [15,16]. The *m/z* 18, 60 and 72 ion signal temperature profiles in Fig. 5 have similar shapes. In contrast, the *m/z* 91 ion signal temperature profile exhibits a different shape with greater ion signal at high temperatures. Fig. 6 shows isoconversion effective activation energies derived from TG-MS analyses of PVB. Activation energies were calculated at 1% intervals from 1 to 99% conversion. To facilitate comparisons, isoconversion activation energies are plotted vs. the sample temperature at which the isoconversion point occurred when PVB was heated at 10 K/min. The broken lines in Fig. 6 plots represent conversions as a function of isoconversion temperature for PVB heated at 10 K/min. The mass-loss isoconversion curve (Fig. 6(e)) exhibits stepwise increases indicative of sequential reaction processes with increasing activation energies. Inspection of *m/z* 18 and 60 isoconversion activation energy curves (Fig. 6(a) and (b)) suggests that processes responsible for evolution of water and acetic acid below 600 K were characterized by unrealistically low activation energies. These low activation energies are not apparent in the mass-loss activation energy curve shown in Fig. 6(e). Apparently, errors in species-specific activation energies for water and acetic-acid evolutions at low conversions resulted from the low signal-to-noise ratios of mass spectra acquired during these regions of the evolution profiles. Between 620 and 700 K, isoconversion activation energies for water, acetic acid, and butanal evolution increased dramatically. Activation energies calculated for this temperature range characterize processes that result in the decomposition of most of the polymer (Fig. 5) and were derived from mass spectra with higher signal-to-noise ratios than those recorded at evolution profile extremes. Above 700 K, isoconversion activation energies for water, acetic acid, and butanal evolution decreased. These activation-energy changes were accompanied by significant volatile alkyl aromatics production. Apparently, water, acetic acid, and butanal evolved more easily when alkyl aromatics were also produced. Isoconversion activation energies representing alkyl aromatics evolutions (Fig. 6(d)) remained relatively constant between 625 and 775 K. Alkyl aromatics were formed from polyene segments created by initial PVB decomposition reactions [16]. Consequently, the *m/z* 91 ion signal temperature profile in Fig. 5 and the isoconversion activation energy profile in Fig. 6(d) are shifted to higher temperatures relative to those for the primary volatile decomposition products.

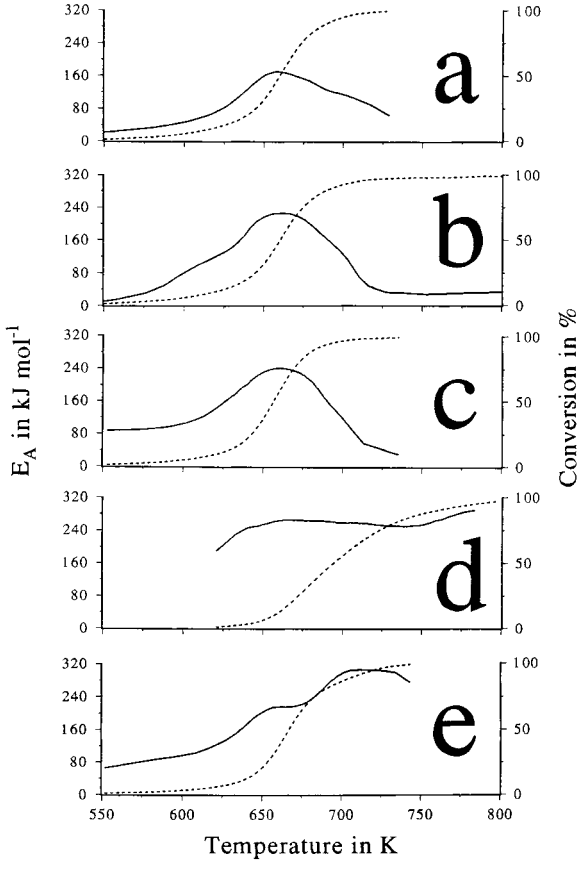

Fig. 6. TG-MS PVB decomposition conversions (broken lines) and isoconversions effective activation energies derived from: (a) *m/z* 18 (water); (b) *m/z* 60 (acetic acid); (c) *m/z* 72 (butanal); (d) *m/z* 91 (alkyl aromatics); and (e) mass loss (solid lines).

The mass-loss derived isoconversion activation energy profile in Fig. 6(e) exhibits three distinct regions that can be correlated to species-specific isoconversion activation energy profiles. Below 700 K, mass-loss derived activation energies were determined primarily by butanal evolution, which was the most abundant volatile product, and by water and acetic-acid evolutions. Like the butanal activation energy plot shown in Fig. 6(c), the mass-loss derived curve in Fig. 6(e) exhibits a gradual increase from ca. 80 to 150 kJ mol^{-1} between 550 and 625 K followed by an

increase to 220 kJ mol^{-1} near 650 K. The ca. 20 kJ mol^{-1} reduction in the mass-loss derived activation energy at 650 K, compared to the acetic-acid and butanal specific activation energies, can be explained by contributions to mass loss by water evolution ($\sim$160 kJ mol^{-1}) at this temperature. As illustrated by Fig. 5, *m/z* 91 was an abundant ion in TG-MS mass spectra acquired above 700 K, suggesting that volatile alkyl aromatics production largely determined mass-loss derived activation energies at these temperatures. However, unlike the *m/z* 18, 60 and 72 mass-spectral ion signal temperature profiles, the *m/z* 91 ion signal temperature profile was not representative of a single species. Differences in the yields of individual alkyl aromatics and in the relative abundance of *m/z* 91 in the mass spectra of these species were likely responsible for the ca. 50 kJ mol^{-1} differences between effective activation energies derived from mass-loss and mass-spectral ion signal temperature profiles between 700 and 750 K (Fig. 6(d) and (e)).

4. Conclusions

The calcium oxalate monohydrate TG-MS results described here confirm that mass-spectral information can be used to calculate isoconversion effective activation energies. However, to obtain accurate activation energies, the TG-MS interface and mass-spectrometer ion source must provide mass-spectral ion signal temperature profiles that are consistent with species-specific evolution profiles. This requires efficient purging of the TG furnace tube, compensation for the delay between formation of volatile products in the TG furnace and detecting them in the mass-spectrometer ion source, and rapid removal of volatiles by the mass-spectrometer vacuum system. Isoconversion effective activation energies derived from TG mass-loss data for PVB revealed three distinct decomposition regions but provided little insight into specific reaction mechanisms. In contrast, species-specific isoconversion activation energies derived from mass-spectral data provided information regarding formation of specific products and reflected the complexities and relationships between decomposition processes.

Acknowledgements

Financial support for this work from the National Science Foundation (CTS-9509240) is gratefully acknowledged.

References

[1] T. Ozawa, Bull. Chem. Soc. Jpn. 38 (1965) 1881.
[2] S.V. Vyazovkin, A.I. Lesnikovich, Thermochim. Acta 165 (1990) 11.
[3] S.V. Vyazovkin, A.I. Lesnikovich, Thermochim. Acta 165 (1990) 273.
[4] S. Vyazovkin, Int. J. Chem. Kinet. 28 (1996) 95.
[5] M.S. Kelsey, Amer. Lab. (1) (1996) 13.
[6] S. Vyazovkin, V. Goryachko, V. Bogdanova, V. Guslev, Thermochim. Acta 215 (1993) 325.
[7] S.V. Vyazovkin, V.V. Bogdanova, I.A. Klimovtsova, A.I. Lesnikovich, J. Appl. Polym. Sci. 42 (1991) 2095.
[8] S.V. Vyazovkin, V.V. Bogdanova, I.A. Klimovtsova, A.I. Lesnikovich, J. Appl. Polym. Sci. 44 (1992) 2157.
[9] S. Vyazovkin, W. Linert, Int. J. Chem. Kinet. 27 (1995) 73.
[10] S.V. Vyazovkin, A.I. Lesnikovich, V.A. Lyutsko, Thermochim. Acta 165 (1990) 17.
[11] S.V. Levchik, E.E. Bolvanovich, A.I. Lesnikovich, O.A. Ivashkevich, P.N. Gaponik, S.V. Vyazovkin, Thermochim. Acta 168 (1990) 211.
[12] T. Ozawa, K. Kanari, Thermochim. Acta 234 (1994) 41.
[13] R.L. White, J. Ai, Appl. Spectrosc. 46 (1992) 93.
[14] T. Ozawa, Thermochim. Acta 203 (1992) 159.
[15] R.L. White, J. Ai, Chem. Mater. 4 (1992) 233.
[16] A. Nair, R.L. White, J. Appl. Polym. Sci. 60 (1996) 1901.